Research on optimization and evaluation method of heavy-haul train cyclic braking manipulation

Wen He, Chongyi Chang and Lan Li
Railway Science and Technology Research and Development Center, China Academy of Railway Sciences Corporation Limited, Beijing, China, and
Yupan Song
China Railway Taiyuan Group Corporation Limited, China Railway Group Ltd, Beijing, China

Received 22 November 2024
Revised 6 January 2025
Accepted 6 January 2025

Abstract

Purpose – The study aims to build a high-precision longitudinal dynamics model for heavy-haul trains and validate it with line test data, present an optimization method for multi-stage cyclic brakes based on the model and conduct a multi-objective detailed evaluation of the driver's manipulation during cyclic braking.

Design/methodology/approach – The high-precision longitudinal train dynamics model was established and verified by the cyclic braking test data of the 20,000 t heavy-haul combination train on the long and steep downgrade. Then the genetic algorithm is employed for optimization subsequent to decoupling multiple cyclic braking procedures, with due consideration of driver operation rules. For evaluation, key manipulation assessments in the scenario are prioritized, supplemented by multi-objective evaluation requirements, and the computational model is employed for detailed evaluation analysis.

Findings – Based on the model, experimental data reveal that the probability of longitudinal force error being less than 64.6 kN is approximately 68%, 95% for less than 129.2 kN and 99.7% for less than 193.8 kN. Upon optimizing manipulations during the cyclic braking, the maximum reduction in coupler force spans from 21% ~ 23.9%. And the evaluation scores imply that a proper elevation of the releasing speed favors safety. A high electric braking force, although beneficial to some extent for energy-saving, is detrimental to reducing coupler force.

Originality/value – The results will provide a theoretical basis and practical guidance for further ensuring the safety and energy-efficient operation of heavy haul trains on long downhill sections and improving the operational quality of heavy-haul trains.

Keywords Heavy-haul trains, Longitudinal train dynamics, Cyclic brake, Manipulation optimization, Detailed manipulation evaluation

Paper type Research paper

1. Introduction

With the development of heavy-haul railways around the world, heavy-haul transportation technology has entered a new stage of development. However, due to the continuous increase in the tonnage of heavy-haul trains and the longer train formations, the difficulty of operating heavy-haul combined trains has further increased. The long downhill sections, as critical segments of the railway line, present complex force conditions for each car in the heavy-haul combined train, resulting in high operational difficulty. How heavy-haul trains can safely and efficiently traverse long downhill sections is a significant issue in the fields of longitudinal

This study has been subsidized by Science and Technology Development Project Agreement/Contract, China State Railway Group Co., Ltd (No. J2022J009) and China Academy of Railway Sciences Co., Ltd (No. 2024YJ124), to which the authors hereby express their appreciation.

Railway Sciences
Vol. 4 No. 2, 2025
pp. 231-248
Emerald Publishing Limited
e-ISSN: 2755-0915
p-ISSN: 2755-0907
DOI 10.1108/RS-11-2024-0048

train dynamics (LTD) and train operation optimization. The commonly used method in actual operations is long-distance cyclic braking control, which involves alternating between air braking and releasing, along with electric braking to assist in speed control. However, cyclic braking involves multiple operational steps and requires precise control, making it difficult for drivers to master the timing and level for various operations, which can easily lead to excessive longitudinal forces. This may result in mid-route stops, severely affecting transportation efficiency; in more severe cases, it can directly lead to train coupler failures and derailments, posing a threat to transportation safety.

The most effective measure to address this issue is to optimize train manipulation based on the theory of LTD, seeking the optimal timing for braking or releasing and the level of the handle level. Through a detailed evaluation and analysis of train manipulation, feedback is provided to drivers regarding current manipulation issues, helping them to timely improve train operation and enhance operational quality. In the field of theoretical research on LTD simulation, Cole and Sun (2006) and Wu, Spiryagin, and Cole (2015, 2016), Wu *et al.* (2017, 2021) conducted in-depth analyses of the LTD performance and fatigue wear of common draft gear system types through comparative simulations. They also conducted more detailed studies on the systematic theory of LTD and the integration of air brake systems with parallel computing. Chang and Wang (2006) established a LTD simulation model for heavy-haul trains, studying the variation patterns of longitudinal forces in a 20,000-ton combined train under different delay times and initial braking speeds, and analyzing the longitudinal force patterns of a 40,000-ton ∼ 120,000-ton heavy-haul train under the influences of factors such as train composition length, wireless synchronization control delay of locomotives, and gradient differences on long downhill slopes (Chang, Guo, He, & Liu, 2023). Wei and Hu (2011, 2012) established a joint simulation model of the train air brake system and LTD, conducting systematic and in-depth research on the air brake system of heavy-haul combined trains, longitudinal impulse variations, and key influencing factors. In the area of manipulation optimization and evaluation research, Domanov, Nekhaev, and Cheremisin (2021). optimized energy-saving operations of trains using directed graph theory, Yu, Huang, and Wang (2018) optimized manipulation for safety and speed operations on long downhill slopes based on particle swarm algorithms, and Zhuan and Xia (2007) conducted multi-objective optimization for heavy-haul trains equipped with electronically controlled pneumatic braking devices, such as targeting speed tracking, energy consumption, safety and stability objectives. Existing research has rarely focused on optimizing specific manipulation details, and the optimization for long-distance operations results in excessive computation time, which lacking engineering advantages.

The research establishes a numerical model of the draft gear system that combines measured data with mechanical principles and a fluid model of the train air braking system based on airflow theory. The single-step balance iterative method is applied in the Newmark-β integral format, thereby creating a high-precision computational model for the LTD. Based on this computational model, the optimization method reasonably considers the constraints of excellent driver operation rules in the manipulation optimization process. After decoupling the multiple cycles of braking operations, a heuristic algorithm is employed to optimize the process, reducing computation time and obtaining feasible optimized operations. The evaluation of operations primarily focuses on key operational assessments within the scenario, supplemented by multi-objective evaluation requirements. The high-precision computational model of LTD is applied to the reproduction and analysis of train operations, achieving detailed evaluation and feedback. The research methods and results can provide theoretical insights for modeling key sub-models of LTD, offering important references to ensure safe and energy-efficient operation of heavy-haul trains on long downhill slopes and to enhance the operational quality of heavy-haul trains.

2. High-precision computational model of longitudinal train dynamics

Based on the traditional theory of LTD, the key points for achieving high-precision calculations are as follows:

(1) Updating and adjusting key simulation parameters to effectively improve cumulative simulation errors;

(2) Accurately simulating the working characteristics of various major subsystems of heavy-haul train formations (such as locomotive traction or electric braking characteristics, air brake system working characteristics, and draft gear device working characteristics, etc.);

(3) Correctly handling the coupling control relationships of various subsystems of the train (such as the instruction delay transmission process of the distributed wireless control system for combined train, and the coupling control process between the wireless control system and the air brake system, etc.);

(4) High-precision multi-body dynamics numerical integration methods;

Based on the high-precision calculation requirements of LTD, more realistic and lower-error computational methods are adopted for the key sub-models of the coupler buffer device, air brake system, and numerical computation methods.

2.1 Detailed numerical simulation of draft gear system

The numerical simulation accuracy of the draft gear device is directly related to the calculation accuracy of the LTD. In the modeling of buffers, issues such as nonlinear loading and unloading processes, velocity damping, peak characteristics, and locking stiffness introduce significant nonlinear variations in the buffer. Additionally, due to the instability of the dry friction mechanical structure of steel, the impact test results of steel friction buffers generally exhibit considerable dispersion and disorder. Therefore, to accurately model the buffer, it is essential to fully consider these issues. Based on the proposed model in the relevant literature (Chang, Wang, Ma, & Zhang, 2006), the expression formula for nonlinear characteristics is improved, and issues such as locking stiffness are taken into account, leading to the proposal of an improved numerical integration model for the draft gear device. For a buffer at a specific position, the expression (Fancher, Ervin, MacAdam, & Winkler, 1980) for the coupler force is in the form of formula (1):

$$F_c(t) = f_{edge} + \left(F_c(t-\Delta t) - f_{edge}\right) \times e^{\frac{-|dx(t)-dx(t-\Delta t)|}{h_5}} \tag{1}$$

In the formula, $F_c(t-\Delta t)$ and $F_c(t)$ are the coupler force at $t-\Delta t$ and t, f_{edge} is the buffer edge loading or unloading force, $dx(t)$ and $dx(t-\Delta t)$ are the relative displacement at t and $t-\Delta t$, h_5 is the numerical integration control coefficient.

Considering the buffer locking stiffness, the modified coupler force $F_c{}'(t)$ is calculated according to formula (2).

$$\begin{cases} KT = \dfrac{F_c(t) - F_c(t-\Delta t)}{dx(t) - dx(t-\Delta t)} \\ F_c{}'(t) = F_c(t-\Delta t) + (F_c(t) - F_c(t-\Delta t)) \cdot \dfrac{|dv(t)|}{ve}, KT > KT_{lock} \end{cases} \tag{2}$$

In the formula, KT is the instantaneous stiffness of the buffer at t, KT_{lock} is the locking stiffness which is measured experimentally to be approximately 8e4 kN/m (Wu *et al.*, 2015), $dv(t)$ is the relative velocity of the coupler before and after the locomotive at t, and ve is the critical transition velocity.

$$f_{edge} = \begin{cases} f_{load}, & dx(t) \geq dx(t-\Delta t) \\ f_{unload}, & dx(t) < dx(t-\Delta t) \end{cases} \tag{3}$$

In the formula, f_{load} and f_{unload} represents the loading and unloading force under the buffer dynamic loading characteristics constructed using a large amount of impact test data (in this construction step, the coupler clearance and preload are considered).

During the loading process of the steel friction buffer, non-linear impact peak are more likely to occur as the impact speed increases. Therefore, it is necessary to superimpose the viscous friction force $f_{viscous}$ on the basis of dynamic loading characteristics, as shown in formulas (4) and (5), h_3 and h_4 are the adjustment coefficient for the viscous friction force.

$$f_{edge} = \begin{cases} f_{load} + f_{viscous}, & dx(t) \geq dx(t-\Delta t) \\ f_{unload}, & dx(t) < dx(t-\Delta t) \end{cases} \tag{4}$$

$$f_{viscous} = h_3 \cdot f_{load} \cdot e^{|dx(t)| - h_4 \cdot |dv(t)|} \tag{5}$$

When constructing elastic polymer dampers, the damping effect should be considered. Therefore, the damping force $f_{damping}$ is superimposed on the basis of the static pressure test characteristics of the buffer, as shown in formulas (6) and (7).

$$f_{edge} = \begin{cases} f_{load} + f_{damping}, & dx(t) \geq dx(t-\Delta t) \\ f_{unload}, & dx(t) < dx(t-\Delta t) \end{cases} \tag{6}$$

$$f_{damping} = h_1 \cdot dv(t) \cdot \left(1 - e^{-h_2 \cdot |dx(t)|}\right) \tag{7}$$

2.2 Fluid model of air brake system

When modeling the train air brake system that uses compressed air as the transmission medium, the actual structure of the train air brake system and the air flow process are taken into account to establish an aerodynamic air brake system model based on air flow theory (referred to as the "fluid model").

For the computational solution of the actual air flow process, the characteristic line method is used to establish the fluid model, which mainly divides the actual air brake system into calculation steps such as air pipeline state calculation, boundary processing, system cylinder pressure calculation, and valve core position judgment. Since the temperature rise during the actual use of the air brake system is not significant, the flow in the pipe is treated as one-dimensional, frictional, and isothermal flow, with the N-S flow equations as shown in equation (8).

$$\begin{aligned} &\frac{\partial \rho}{\partial t} + \rho \frac{\partial u}{\partial x} + u \frac{\partial \rho}{\partial x} = 0 \\ &\frac{\partial u}{\partial t} + u \frac{\partial u}{\partial x} + \frac{1}{\rho} \frac{\partial p}{\partial x} + f \frac{u^2}{2} \frac{u}{|u|} \frac{4}{D} = 0 \end{aligned}, \tag{8}$$

In the equation (8), ρ, u, p, D, x, t, f represents air density, air flow velocity, gas pressure, hydraulic diameter, displacement, time and pipe wall friction coefficient respectively.

The N-S equations are transformed into Riemann variables based on the characteristic line theory, and the increment of Riemann variables between different time steps is calculated as shown in equation (9).

$$d\lambda = -\frac{k-1}{2}\frac{2fx_{\text{ref}}}{D}\left(\frac{\lambda-\beta}{k-1}\right)^2\frac{(\lambda-\beta)}{|\lambda-\beta|}\left\{1-\frac{2(\lambda-\beta)}{(\lambda+\beta)}\right\}dZ, \tag{9}$$

In the equation (9), k is the adiabatic coefficient; x_{ref} is the reference length.

The gas flow rate between the cylinder and the external gas is calculated using equation (10) (Wu *et al.*, 2017).

$$\dot{m} = \begin{cases} \dfrac{P_1A_e}{a_1}\left\{\left(\dfrac{2k^2}{k-1}\right)\left(\dfrac{P_2}{P_1}\right)^{2/k}\left[1-\left(\dfrac{P_2}{P_1}\right)^{(k-1)/k}\right]\right\}\dfrac{1}{2} & \dfrac{P_2}{P_1} > \left(\dfrac{2k}{k+1}\right)^{\frac{k}{k-1}} \text{(Subsonic flow)} \\ \dfrac{P_1A_e}{a_1}k\left(\dfrac{2}{k+1}\right)^{(k+1)/[2(k-1)]} & \dfrac{P_2}{P_1} \le \left(\dfrac{2k}{k+1}\right)^{\frac{k}{k-1}} \text{(Choked flow)} \end{cases}, \tag{10}$$

In the equation (10), P_1 and P_2 are the pressures on both sides of the opening, A_e is the opening area.

For the 120/120-1 valve, the main calculations involve the positions of the main valve piston and the slide valve piston, which can determine the specific operating conditions of the brake machine (such as releasing, deceleration releasing, braking, emergency braking, and holding pressure, etc.). The components of the 120/120-1 valve are simplified as shown in Figure 1, and by establishing the connectivity relationships and aperture opening logic in sequence, a fluid model can be developed.

Taking the "1 + 1+End-of-train (EOT)" combination train formation as an example, the number of freight cars within the unit formation is 108, and the freight cars use 120 valves. Using the most common initial braking operation as an example, the hardware equipment consists of an Intel i7-12700H 14-core 2.3GHz processor and 16GB of memory. A numerical program simulation is written in C++ language, and the 216 freight cars within the formation are calculated sequentially. In the calculation, the main grid length is taken as 0.675 m, and the branch grid length is taken as 0.3 m. The simulation results are compared with experimental data as shown in Figure 2. It can be seen that the fluid model can accurately reflect the various

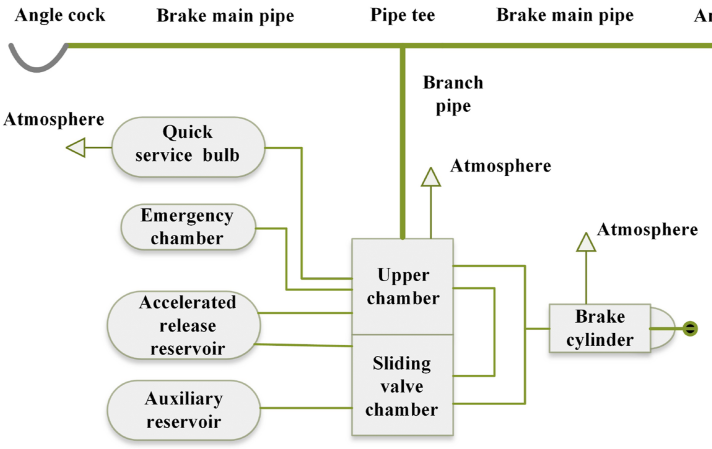

Source(s): Authors' own work

Figure 1. The components of the 120/120-1 valve'

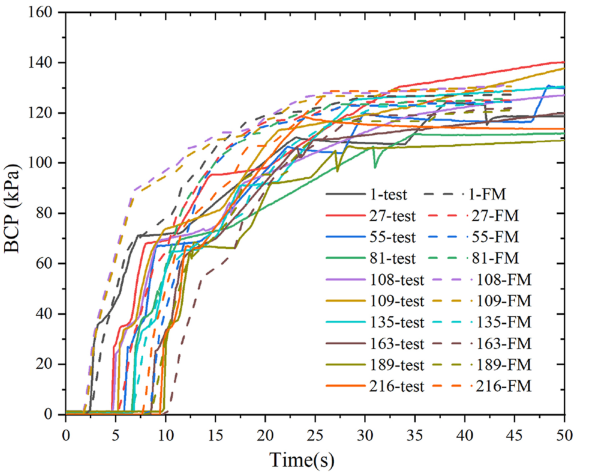

Source(s): Authors' own work

Figure 2. Comparison of fluid model results with test data

working characteristics such as pressure boosting and pressure maintenance of the air brake system, as well as the impact of specific structural features of the air brake system. The transmission of braking wave speed and the calculation of the final equilibrium pressure are relatively accurate.

2.3 Explicit numerical integration method for multibody systems

The LTD model, as shown in Figure 3, first considers a single locomotive or vehicle as a separate car. A single car has one degree of freedom in the longitudinal direction (He, Chang, Wang, & Guo, 2024). By analyzing the longitudinal forces acting on the single car, as shown in Figure 4, its longitudinal dynamic equation is given by formula (11):

$$m_i\ddot{u}_i = F_{Ti}(-F_{Di}) - F_{Bi} - F_{wi} + F_{c(i-1)} - F_{ci}\,(i = 0, 1, \cdots, n) \tag{11}$$

In the formula (11), $F_{c(i-1)}$, F_{ci} represents the front and rear coupler force of the ith vehicle, m_i is the mass of the ith vehicle, u_i is the displacement of the ith vehicle, F_{Ti} is the traction force of the ith vehicle (acting on the locomotive), F_{Di} is the regenerative braking force of the ith vehicle (acting on the locomotive), F_{Bi} is the air braking force of the ith vehicle, and F_{wi} is the total resistance of the ith vehicle.

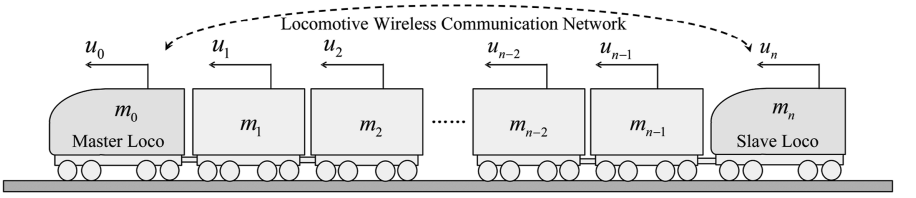

Source(s): Authors' own work

Figure 3. Train simulation model in LTD

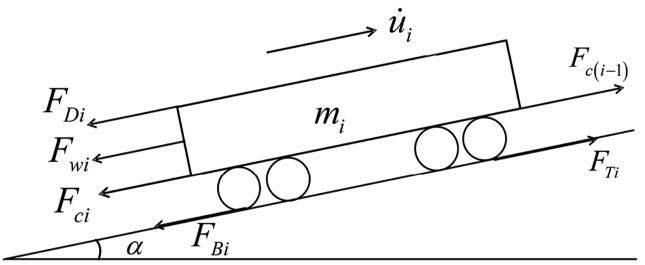

Source(s): Authors' own work

Figure 4. Longitudinal analysis of single car

Due to the presence of various nonlinear factors in the longitudinal dynamics equations of trains, which complicate the computation, the research aims to ensure computational accuracy. Based on the Newmark-β numerical integration method (Newmark, 1959), the step-by-step integration method is further applied to the response calculation of nonlinear equations. At $t + \Delta t$, the system incremental balance equation is given by equation (12):

$$M(\ddot{u}_{t+\Delta t} - \ddot{u}_t) + K_T(\Delta u_t) = F_{t+\Delta t} - F_t, \tag{12}$$

In the equation (12), M represents the mass matrix, K_T represents the stiffness matrix; $\ddot{u}_t$ and $\ddot{u}_{t+\Delta t}$ are the acceleration matrices at t and $t + \Delta t$, Δu_t represents the relative displacement at t; F_t and $F_{t+\Delta t}$ are the force vectors resisting deformation at t and $t + \Delta t$.

Since K_T varies with the iterative process, an approximate solution is only found when it changes to the final equilibrium position. Therefore, the core idea of the equilibrium iteration method is to approximate with linear results and calculate the resulting unbalanced forces, repeating the iteration until no unbalanced forces are generated, as shown in Figure 5. Ultimately, the method of stepwise iteration to eliminate unbalanced forces is used to solve the nonlinear equations of LTD.

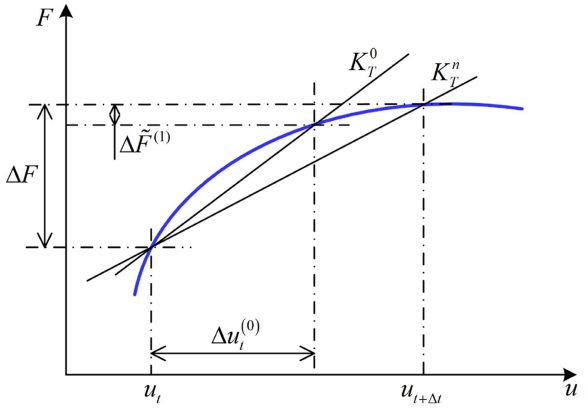

Source(s): Authors' own work

Figure 5. Incremental step iteration process of stepwise integration

3. Verification of test data from long downhill sections

The cyclic braking operation in long downhill sections is an important feature that distinguishes heavy-haul lines from general freight lines. A segment of measured data from a heavy-haul line in China is selected to compare and analyze the calculation accuracy of the LTD model. The basic running resistance coefficient is adjusted and optimized using a heuristic algorithm, taking $a_l = 1.0473$, $b_l = 0.0028$, $c_l = 0.0002244$, $a_w = 0.4662$, $b_w = 0.0021$, $c_w = 0.000061$. The method is based on the actual operation sequence data of a train in a section without air braking process. Through the actual data, the tractive force or regenerative force of the current locomotive is dynamically updated, and then the basic running resistance of the train is taken as the independent variable. With the objective function being to minimize the mean value of speed errors, the optimal basic resistance coefficient is finally solved through the genetic algorithm.

The selected line has a total length of 13 km (K44 + 000~K57 + 000), with a longitudinal slope of −9% to −12%, a minimum curve radius of 500m, and no electric phase separation sections (Yao, 2016). The train group parameters are shown in Table 1. The train operation sequence is based on the actual driver's operation sequence, and the computing hardware consists of an Intel i7-12700H 14-core processor and memory.

Through the comparative analysis of simulation data and measured data in Figure 6, it can be seen that the average calculation error of the simulation speed is less than 2 km/h, with a maximum speed error of 3.72 km/h. The calculation results of the simulation model at all test locations closely match the actual variation trend of the coupler force, demonstrating good simulation of the severe impact during the transition of key operating conditions in cyclic braking. A normal distribution analysis of the longitudinal force calculation error distribution shows that the probability of the longitudinal force calculation error being less than 64.6 kN is approximately 68%, a 95% probability less than 129.2kN, and a 99.7% probability less than 193.8kN, indicating good calculation performance.

4. Optimization method for long downhill cyclic braking operation

When modeling the multi-objective optimization problem of cyclic braking for heavy-haul trains on long slopes, in order to make the optimization solving process more meaningful for engineering, the modeling of the cyclic braking multi-objective optimization problem is based on the constraints of the driver's long-term operational experience. For a typical heavy-haul train's long slope cyclic braking process, as shown in Figure 7, Point A indicates the start of the train entering the long slope section; Point B indicates the start of the first air brake; Point C indicates the start of the release; Point D indicates the start of the second air brake after the release is completed, followed by subsequent release and air braking until the train exits the long slope; Point C' represents the position where the electric brake input before release remains stable until the start of the release; Point C'' indicates the position of the first change in electric brake input after release.

Table 1. Train group parameters

Calculation parameters	Values
Train group form	HXD1 + C80×108 + HXD1 + C80×108 + EOT
Total traction weight	21,000 tons
Buffer type	Locomotive: QKX100; Vehicle: MT-2
Coupling form/coupler clearance	3 vehicles per unit/9.5 mm
Wireless synchronization control delay time	3s

Source(s): Authors' own work

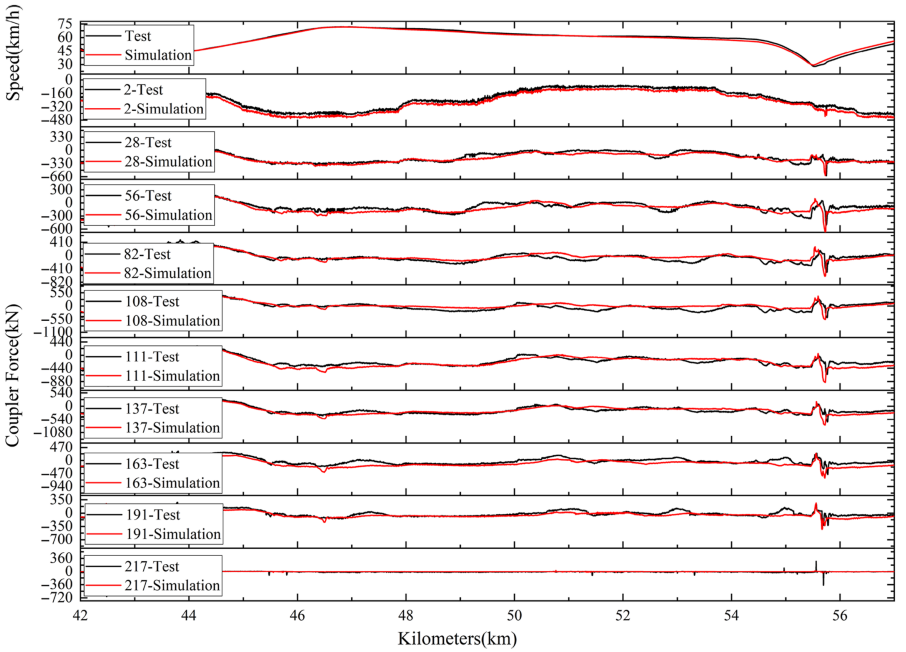

Source(s): Authors' own work

Figure 6. Comparison of coupler force at different test locations

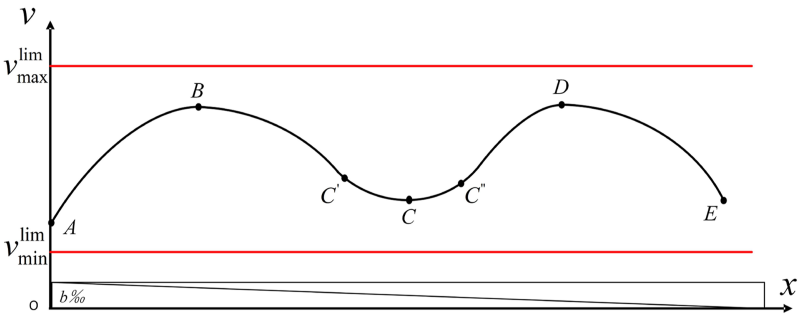

Source(s): Authors' own work

Figure 7. Long downhill cyclic brake of heavy haul trains

4.1 Decomposition of the cyclic braking process

By establishing the relationship between the release time after recharging, average slope value, releasing speed, and electric braking force after a period of release, the global optimization process of multiple cycles during long downhill sections can be decomposed into multiple single brake-release optimization solutions, thereby reducing computational complexity and improving computational efficiency. In the simplification of the cyclic braking process involving multiple brake-release processes, the principle of satisfying the recharging time for the train composition is primarily followed, and based on this, the average passing speed on the

slope is improved. The decomposition process of cyclic braking that includes multiple brake-release processes is as follows:

Step 1: Clarify the magnitude of the pressure reduction used in speed control braking and the corresponding recharging time.

Step 2: Establish an empirical relationship between the release time after recharging, average slope value, releasing speed, and electric braking force after a period of release. According to this empirical relationship, obtain the optimized constraint range for the releasing speed v_C shown in Figure 7 and the values for electric braking force $N_{C''D}$.

Step 3: Optimize the single brake-release process based on a genetic algorithm according to the selected releasing speed range, and the electric braking force $N_{C'C''}, N_{C''D}$ has been obtained. By continuously decomposing and optimizing this process, a cyclic braking that includes multiple processes can be completed.

4.2 Considerations for cyclic braking constraints based on single process

In the single brake-release process, if there are no excessive constraints and limitations, all decision variables can take arbitrary values. Therefore, it is necessary to introduce actual physical system constraints and relevant driver experience constraints, which make the solution of the multi-objective optimization problem reasonable and feasible.

(1) Physical Constraints:

- The electric braking force during the cyclic braking process is less than the maximum electric braking force $N_{\max}$, that is $0 < N_{AD} \leq N_{\max}$.
- The braking pressure reduction P_{BC} is within the commonly used range, that is $50kPa \leq P_{BC} \leq 170kPa$;
- The available recharging time for the train after releasing is greater than the current recharging time under the pressure reduction, that is $t_{release} > t_{\min}^{release}$;

(2) Driver Experience Constraints:

- The speed when starting the air brake is less than the current section speed limit, that is $v_B < v_{\max}^{\lim}$;
- The speed when it begins to release is greater than the minimum releasing speed, that is $v_C > v_{\min}^{\lim}$;
- During the operation of the train, the electric brake force should avoid using the full level as much as possible, that is $N_{AD} < N_{\max}$;
- The frequency of changing the electric brake force during the operation of the train should be kept as low as possible; therefore, the electric brake force during a single brake-release process is constrained to three constant level parts of $N_{BC'}, N_{C'C''}, N_{C''D}$;
- The electric brake force $N_{C'C''}$ remains unchanged over a certain distance before and after releasing.
- Priority of pressure reduction should be given to the most commonly used by the driver, P_{BC} preferentially uses 50 kPa.;
- The selection of air brake locations and release locations should avoid complex gradient sections as much as possible to prevent the longitudinal coupler force from exceeding the maximum pulling force limit $F_{\max}^{tensile}$ and the maximum pushing force limit $F_{\max}^{compress}$, that is $F_{\max}^{compress} \leq F_{coupler} \leq F_{\max}^{tensile}$;

4.3 Construction of the objective function for the cyclic braking process

Taking running time and operational safety as the basic guiding objectives, the objective function is composed as shown in formula (13),

$$J = \alpha_1 \left| T_{run} - T_{goal} \right| + \alpha_2 \left| F_{\text{cmax}}^{tensile} \right| + \alpha_3 \left| F_{\text{cmax}}^{compress} \right| \tag{13}$$

In the equation (13), $F_{\text{cmax}}^{tensile}$ represents the maximum pulling coupler force during the cyclic braking process, $F_{\text{cmax}}^{compress}$ represents the maximum pressing coupler force during the cyclic braking process, α_1, α_2 and α_3 are the efficiency weight coefficients, maximum pulling force and maximum pressing force weight coefficients, respectively, T_{run} is the actual running time of the train, and T_{goal} is the planned running time of the train.

By solving the minimization objective function within the constraint space, the optimized variable values $v_B, v_C, N_{BC'}, N_{C'C''}$ can be determined.

4.4 Genetic algorithm for multi-objective optimization

For the multi-objective optimization problem of cyclic braking in a single brake-release process, the Genetic Algorithm is employed for global heuristic optimization as shown in Figure 8. In the cyclic braking optimization process, based on the range of decision variables $v_B, v_C, N_{BC'}, N_{C'C''}$, each decision variable can be encoded using 4-bit binary numbers, resulting in each chromosome consisting of 16 bits to represent a group of decision variables. After initializing the solving parameters of the genetic algorithm and the initial population, the value of the objective function is calculated by invoking the LTD model, which serves as the fitness of each generation of the population. In this step, the focus is on efficiency and operational safety, while fully considering physical constraints and driver experience constraints in the LTD solution, thus saving computational resources to align with practical engineering applications. The optimal group of decision variables for the current brake-release process is obtained after optimization. If the train has not exited the long downhill section after completing the current cycle, the optimization for the next cycle will be conducted until the train exits the long downhill segment.

Taking the long downhill section of the Daqin Line from K290 + 000 to K294 + 000 (average gradient −10.5%, minimum curve radius 700m) as the manipulation optimization section, optimization is performed using the aforementioned methods. The simulation calculation of the train group parameters is shown in Table 2.

Select the planned train operating time T_{goal} = 300s; efficiency weight coefficient $\alpha_1 = 10$; maximum coupler force weight coefficient $\alpha_2 = 1$; maximum coupler force weight coefficient $\alpha_3 = 1$; the releasing speed solving range based on the empirical relationship is [30,40] km/h, the electric brake force after releasing is 70% ~ 80%, and the objective function fitness of the genetic algorithm optimization process varies with the evolutionary generation as shown in Figure 9, reaching the minimum value of the objective function fitness after 40 generations.

The final optimized simulation results are shown in Table 3 and Figure 10. The parameters that changed significantly before and after the optimization are the releasing speed, released position, and the electric braking force used before and after the release. When the released speed is increased to 40km/h, the released position is postponed by 300 m, and the electric braking force before and after release is reduced to 13%, the impact of the asynchronous release caused by the propagation of the released wave is weakened, resulting in a decrease of 208kN ~ 245kN in the maximum coupler force of the 20,000-ton heavy-haul train, with a reduction of 21% ~ 23.9%; the maximum amplitude of the coupler force is reduced by 179kN ~ 801kN, with a reduction of 11.5% ~ 36.9%.

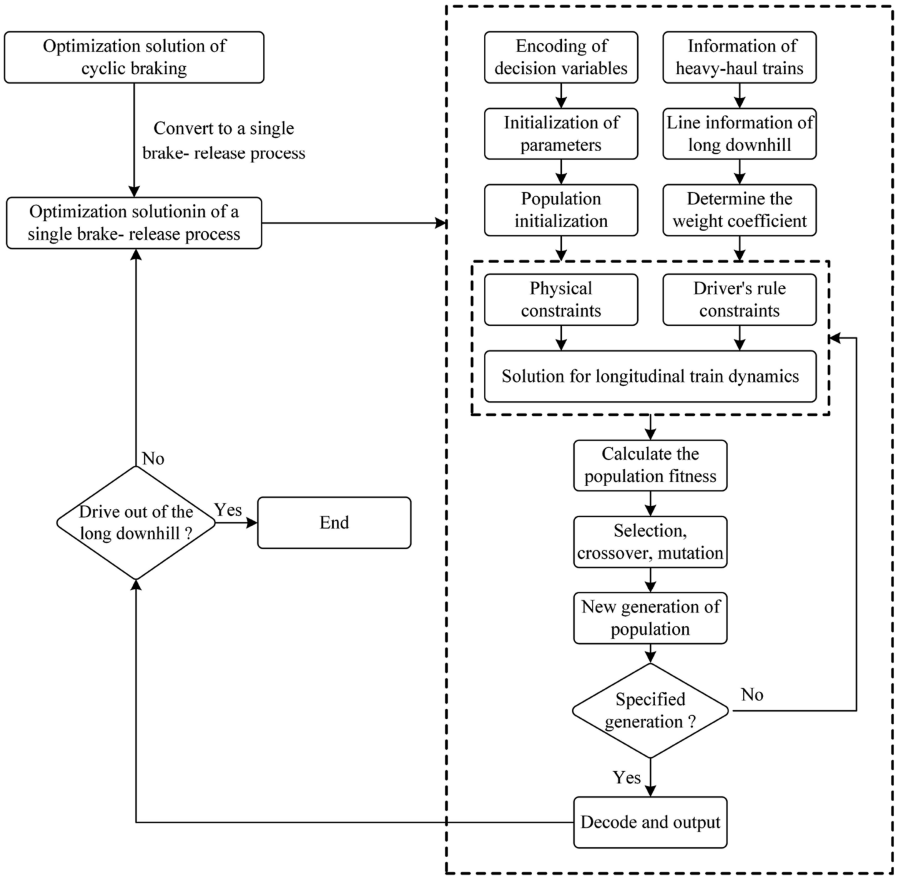

Source(s): Authors' own work

Figure 8. Optimization process of cyclic braking

Table 2. Train group parameters in simulation

Calculation parameters	Values
Train group form	HXD1 + C80×105 + HXD1 + C80×105 + EOT
Total traction weight	20,000 tons
Buffer type	Locomotive: QKX100; Vehicle: MT-2
Coupling form/coupler clearance	3 vehicles per unit/9.5 mm
Wireless synchronization control delay time	3s

Source(s): Authors' own work

5. Evaluation of heavy-haul train operations on long downhill sections

Due to the complexity of the train operation environment, which involves various group types, scene transitions, complex routes, and signal changes, there are challenges in multi-objective trade-offs, multi-parameter considerations, difficulties in obtaining key evaluation parameters, and challenges in quantifying indicators for operational evaluation. The

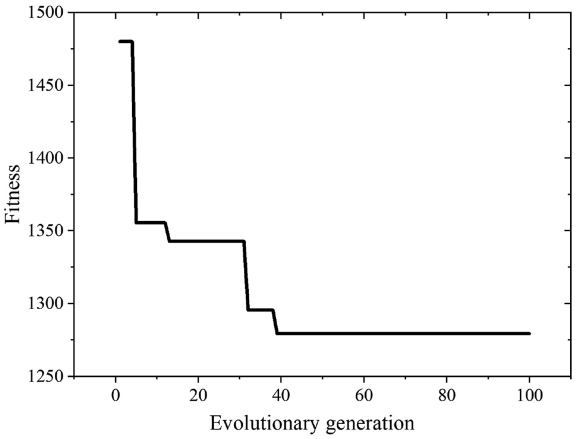

Source(s): Authors' own work

Figure 9. Fitness function curve

Table 3. Comparison of simulation results before and after optimization

Key parameters	Before optimization	Optimized
Braking speed (km/h)	–	63.0
Releasing speed (km/h)	29.6 ~ 30.7	40.0
Release position (km)	K292 + 967	K293 + 260
Electric brake force during air braking	–	40%
Electric brake force before and after releasing	30% ~ 70%	13%
Maximum tensile coupler force (kN)	988 ~ 1,025	780
Maximum compression coupler force (kN)	−322 ~ −1,144	−588
Coupler force amplitude (kN)	1,547 ~ 2,169	1,368

Source(s): Authors' own work

technical difficulties of detailed operational evaluation have led to the current state of train operational evaluation being primarily modular, with limited assistance for driver feedback improvement. The research addresses the need for specific scene operations and multi-objective evaluation by establishing a detailed evaluation method based on key operational evaluations within the scene, supplemented by multi-objective evaluation requirements, through the LTD model. As shown in Figure 11, The key points of this method include train operation scene recognition, identification of key operational points in the scene, trade-offs in multi-objective operational evaluation requirements, and analysis of key operational reproduction.

Taking the typical scenario of a 20,000-ton heavy-haul train running down a long slope as an example, a detailed operational evaluation application is conducted on a segment of a heavy-haul line in China. The average gradient of this segment is −10.5‰, with a minimum curve radius of 800 m. It is assumed that the basic evaluation data is derived from a segment of LKJ running record data shown in Figure 12, and statistical analysis is performed on a total of 21 trips of 3 drivers A, B, and C on this line segment.

The implementation steps of the detailed operational evaluation method are as follows:

(1) Identification of key operational points in the scenario: This involves key operational points such as braking speed/braking position, releasing speed/releasing position,

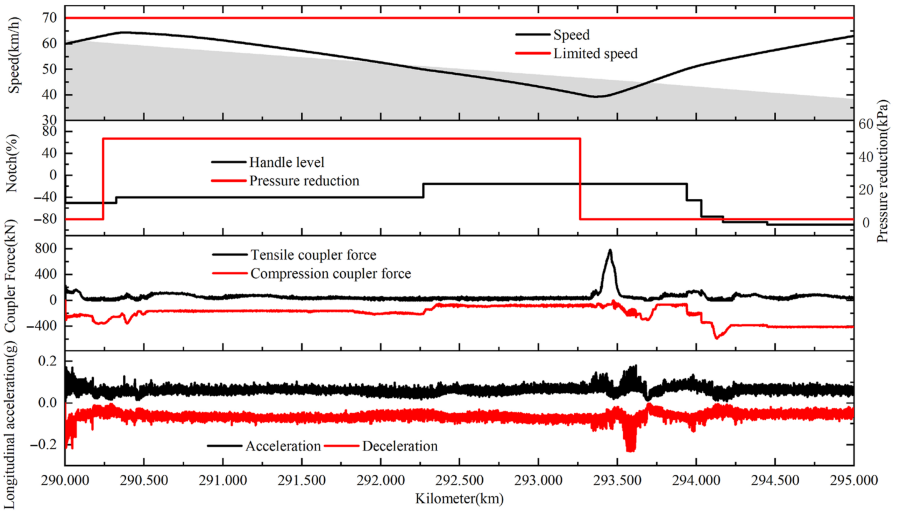

Source(s): Authors' own work

Figure 10. Simulation results of cyclic braking optimization

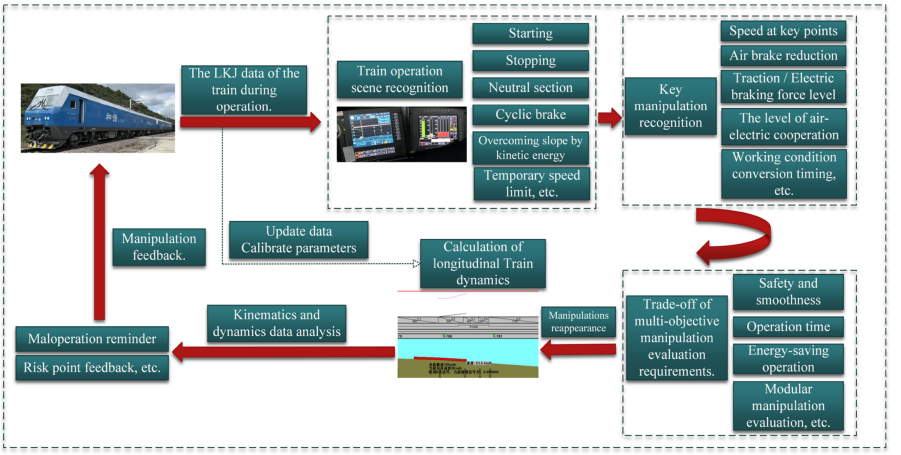

Source(s): Authors' own work

Figure 11. Implementation steps of the detailed train operational evaluation method

braking pressure reduction, and electric braking force before and after release. The braking speed during this cyclic braking process is concentrated between [70, 72] km/h, while the releasing speed is distributed between [39, 57] km/h. The braking and releasing positions are relatively fixed, with the braking position concentrated around K149 + 000 and the releasing position distributed between [K152 + 700 and K153 + 200].

(2) Multi-objective manipulation evaluation demand trade-offs: This involves evaluation demands related to the longitudinal state assessment of trains concerning operational

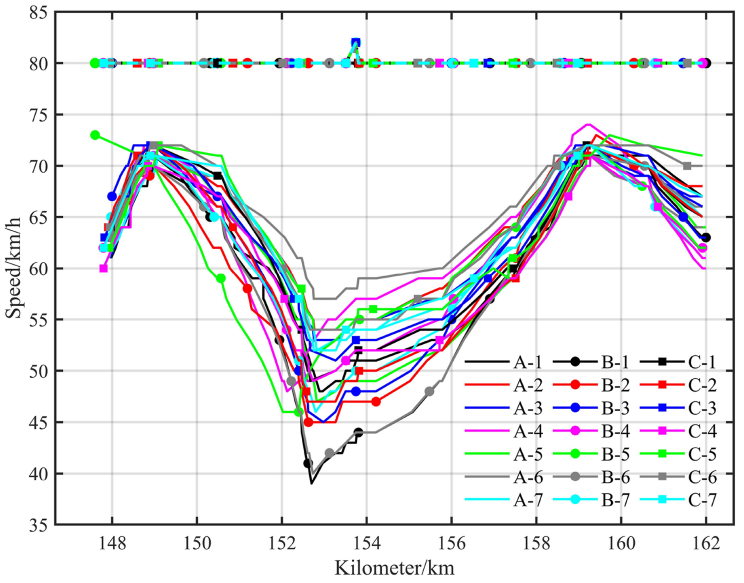

Source(s): Authors' own work

Figure 12. Running data of 21 trips of a heavy-haul train on a long slope

safety, runtime evaluation, segment energy consumption assessment, and whether modular manipulation corresponds, with the total weight of various demands summing to 1;

In long downhill scenarios, train longitudinal state assessment is closely related to safety, with the maximum longitudinal force F_{cmax} of the entire train as the evaluation indicator, and its normalized weight is ω_f; section energy consumption assessment is closely related to energy-saving economics, with the work done by traction/electric braking force in the section W_t as the evaluation indicator, and its normalized weight is ω_e; running time assessment is mainly reflected in whether the dynamic tracking interval between the front and rear of the heavy-haul train meets the requirements, with the running time of the section T_r as the evaluation indicator, and its normalized weight is ω_t; whether it corresponds to modular manipulation mainly reflects whether the driver is familiar with the experience rules of past excellent drivers and whether they are proficient in the overall manipulation of the section, represented by a Boolean value of 0 or 1, with its weight ω_m.

(3) Critical manipulation reproduction analysis: Using known speed, time, and position information, a LTD model is employed to rapidly compute the train's longitudinal impulse level and energy consumption level, to decipher the dynamic data indicators behind the driver's manipulation, and to enable comprehensive and rapid online evaluation and feedback.

By implementing the above refined evaluation and feedback steps, the manipulation evaluation scores for 21 different manipulations in the long downhill section, as shown in Figure 13, can be obtained. Among them, the evaluation that emphasizes safety has its weights allocated as $\omega_f = 0.4$, $\omega_e = 0.25$, $\omega_t = 0.25$, $\omega_m = 0.1$; in the evaluation that emphasizes energy-saving, the weights are allocated as $\omega_f = 0.2$, $\omega_e = 0.5$, $\omega_t = 0.2$, $\omega_m = 0.1$; the normalization method is based on the maximum/minimum values.

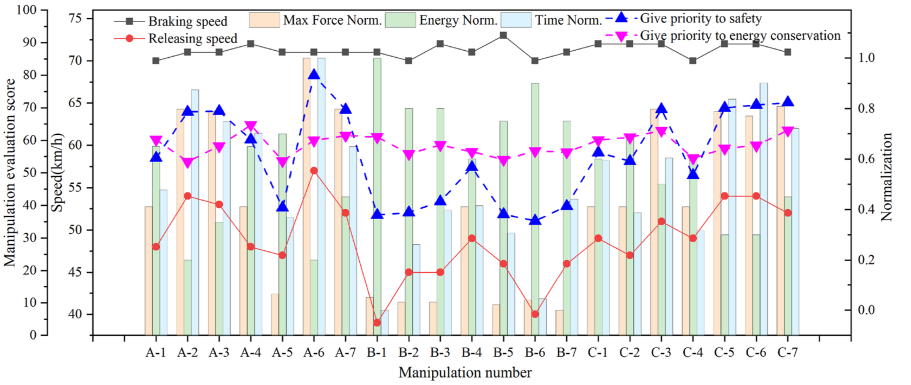

Source(s): Authors' own work

Figure 13. Manipulation evaluation

Analysis of feedback from the manipulation evaluation scores shows that for a 20,000-ton heavy-haul combined train operating in long downhill scenarios, different manipulation conditions yield different scores when evaluated with varying weightings. When safety is prioritized, the weight of the maximum longitudinal force is higher than that of other evaluation indicators, and the evaluation score is closely related to the train's downhill releasing speed, which is approximately positively correlated with the train state during braking release. When energy efficiency is prioritized, It can be intuitively understood that since the locomotive cannot enter the traction state during cyclic braking, the work done by the regenerative braking force becomes the main factor affecting energy consumption. The evaluation score is significantly linked to the amount of electric braking force and the running speed, requiring particular attention to these critical manipulation points by the driver.

From the scoring feedback, it is evident that under the premise of ensuring sufficient recharging time, appropriately increasing the releasing speed is conducive to safe operation. Excessive electric braking force is not conducive to reducing coupler forces but offers certain advantages for energy-efficient operation. The evaluation feedback results align with the conclusions of the aforementioned manipulation optimization. Therefore, conducting detailed manipulation evaluation feedback based on LTD calculations can provide timely and reasonable manipulation suggestions to drivers during operation, which is beneficial for improving manipulation performance.

6. Conclusion

(1) By improving the modeling methods of draft gear systems and the air braking system, and applying a single-step balanced iteration calculation method in the Newmark-β integration format, a high-precision calculation model for the longitudinal dynamics of heavy-haul trains is established, with a comparison of $-9\% \sim -12\%$ against the test data on long downhill sections. The maximum simulation speed error is 3.72km/h, the longitudinal force error has a probability of 68% being less than 64.6kN, with a probability of 95% being less than 129.2kN, and a probability of 99.7% being less than 193.8kN.

(2) In the optimization method for long downhill manipulation, the driver's manipulation rules are reasonably considered to reduce the optimization solution space, and after decoupling multiple cyclic braking processes, a genetic algorithm is used for

optimization. Taking the long downhill section with an average gradient of −10.5% on the Daqing Line as the optimization zone, the optimization of manipulation increases the releasing speed to 40km/h, delays the releasing point by 300 m, and reduces the electric braking force before and after the release to 13%. The maximum coupler force reduction for a 20,000-ton heavy-haul combined train is 21% to 23.9%; the maximum amplitude reduction of the coupler force is 11.5% to 36.9%.

(3) In the detailed manipulation evaluation, the focus is on the manipulation evaluation of key points within the scene, supplemented by the demand for multi-objective evaluation. The high-precision calculation model of LTD is applied to the train manipulation recurrence analysis for detailed evaluation and feedback. Taking the 21 actual operation data of a 20,000-ton heavy-haul combined train running on a long downhill slope of −10.5% as an example, the detailed manipulation evaluation method conducts scoring analysis from the perspectives of safety and energy-saving operation. The scoring results show that under the premise of ensuring sufficient recharging time, appropriately increasing the releasing speed is conducive to safe operation. Although excessive electric braking force is not conducive to reducing coupler forces, it has certain advantages for energy-saving operation.

References

Chang, C., Guo, G., He, W., & Liu, Z. (2023). Simulation study on the influence of longitudinal dynamic force on extreme-long heavy-haul trains. *Railway Sciences*, *2*(4), 495–513. doi: 10.1108/rs-09-2023-0028.

Chang, C., Wang, C., Ma, D., & Zhang, B. (2006). Study on numerical analysis of longitudinal forces of the T20, 000 heavy haul. *Journal of the China Railway Society*, (2), 89–94.

Cole, C., & Sun, Y. Q. (2006). Simulated comparisons of wagon coupler systems in heavy haul trains. *Proceedings of the Institution of Mechanical Engineers, Part F: Journal of Rail and Rapid Transit*, *220*(3), 247–256. doi: 10.1243/09544097jrrt35.

Domanov, K., Nekhaev, V., & Cheremisin, V. (2021). Optimization of operating modes of a train by the haul distance. *Transportation Research Procedia*, *54*, 842–853. doi: 10.1016/j.trpro.2021.02.142.

Fancher, P. S., Ervin, R. D., MacAdam, C. C., & Winkler, C. B. (1980). *Measurement and representation of truck leaf spring*. Ann Arbor: High: Safety Research Institute. The Univof Michigan.

He, W., Chang, C., Wang, J., & Guo, G. (2024). Analysis on key influencing factors of longitudinal force with 30 000 t heavy haul trains in braking conditions. *Journal of the China Railway Society*, 01, 53–59.

Newmark, N. M. (1959). A method of computation for structural dynamics. *Journal of the Engineering Mechanics Division*, *85*(3), 67–94. doi: 10.1061/jmcea3.0000098.

Wei, W., & Yu, Z. (2011). Influence of lag time for slave control locomotive on longitudinal coupler forces of 30 000 t train. *Journal of Traffic and Transportation Engineering*, *11*(2), 39–44.

Wei, W., & Hu, Y. (2012). Influence of train tail exhaust device on longitudinal force of train. *Journal of Traffic and Transportation Engineering*, (5), 43–49+63.

Wu, Q., Cole, C., Spiryagin, M., Chang, C., Wei, W., Ursulyak, L., . . . Cantone, L. (2021). Freight train air brake models. *International Journal of Rail Transportation*, *11*(1), 1–49. doi: 10.1080/23248378.2021.2006808.

Wu, Q., Cole, C., Spiryagin, M., Wang, Y., Ma, W., & Wei, C. (2017). Railway air brake model and parallel computing scheme. *Journal of Computational and Nonlinear Dynamics*, *12*(5), 051017. doi: 10.1115/1.4036421.

Wu, Q., Spiryagin, M., & Cole, C. (2015). Advanced dynamic modelling for friction draft gears. *Vehicle System Dynamics*, *53*(4), 475–492. doi: 10.1080/00423114.2014.1002504.

Wu, Q., Spiryagin, M., & Cole, C. (2016). Longitudinal train dynamics: An overview. *Vehicle System Dynamics*, *54*(12), 1688–1714. doi: 10.1080/00423114.2016.1228988.

Yao, X. (2016). *The test of the 20,000-ton train with a '1+1' marshalling towing 216 C80 freight wagons on the Shuohuang Railway.* Beijing: China Academy of Railway Sciences.

Yu, H., Huang, Y., & Wang, M. (2018). Research on operating strategy based on particle swarm optimization for heavy haul train on long down-slope. In *2018 21st International Conference on Intelligent Transportation Systems (ITSC)* (pp. 2735–2740). IEEE.

Zhuan, X., & Xia, X. (2007). Optimal scheduling and control of heavy haul trains equipped with electronically controlled pneumatic braking systems. *IEEE Transactions on Control Systems Technology, 15*(6), 1159–1166. doi: 10.1109/tcst.2007.899721.

Corresponding author
Wen He can be contacted at: hewen_cars@163.com

Wen He received his M.Eng. Degree from China Academy of Railway Sciences in 2023. Now he is a research assistant in the Railway S&T R&D Center of China Academy of Railway Sciences, focusing on the train dynamics and optimal control.